Journal of Alloys and Compounds 881 (2021) 160511

Contents lists available at ScienceDirect

Journal of Alloys and Compounds

journal homepage: www.elsevier.com/locate/jalcom

A novel hot carrier-induced blue light-emitting device

S. Mutlu[a,*], A. Erol[a], E. Arslan[b,c], E. Ozbay[c,d,e], S.B. Lisesivdin[f], E. Tiras[g]

[a] Department of Physics, Faculty of Science, Istanbul University, Vezneciler, 34134 Istanbul, Turkey
[b] Department of Electrical and Electronics Engineering, Antalya Bilim University, 07190 Antalya, Turkey
[c] Nanotechnology Research Center, Bilkent University, Bilkent, 06800 Ankara, Turkey
[d] Department of Electrical and Electronics Engineering, Bilkent University, Bilkent, 06800 Ankara, Turkey
[e] Department of Physics, Bilkent University, Bilkent, 06800 Ankara, Turkey
[f] Department of Physics, Faculty of Science, Gazi University, Teknikokullar, 06500 Ankara, Turkey
[g] Department of Physics, Faculty of Science, Eskisehir Technical University, Tepebaşı, 26470 Eskişehir, Turkey

ARTICLE INFO

Article history:
Received 30 March 2021
Received in revised form 18 May 2021
Accepted 20 May 2021
Available online 24 May 2021

Keywords:
Top-Hat HELLISH
InGaN/GaN multi quantum well
Field effect
XOR logic
Blue light

ABSTRACT

In this work, an InGaN/GaN multiple quantum well based Top-Hat Hot-Electron Light Emission and Lasing in a Semiconductor Heterostructure (Top-Hat HELLISH) is investigated. A heterojunction structure is designed based on an active InGaN quantum well placed in the n-type GaN region sandwiched by the n- and p-type GaN layers. The four quantum well structure of an InGaN/GaN heterojunction where the Indium ratio is 0.16 has been grown *via* Metal-Organic Chemical Vapor Deposition. In order to create an anisotropic potential distribution of the heterojunction, it is aimed to fabricate TH-HELLISH-GaN device in Top-Hat HELLISH (THH) geometry for four contacts with separate n- and p-channels. High-speed I-V measurements of the device reveal an Ohmic characteristic at both polarities of the applied voltage. Integrated EL measurements reveal the threshold of the applied electric field at around 0.25 kV/cm. The emission wavelength of the device is around 440 ± 1 nm at room temperature.

1. Introduction

A novel light-emitting device based on the hot-electron related operation was proposed in 1994 by N. Balkan [1–4] and called Hot-Electron Light-Emitting and Lasing in Semiconductor Heterostructures (HELLISH). To date, we have witnessed the evolution of HELLISH devices from an LED characteristic to a laser characteristic emitting at 820 nm [5–9], 1300 and 1550 nm [10–12], and at 1300 nm [13]. Furthermore, the anatomy of HELLISH has exhibited a drastic change from HELLISH to Top Hat HELLISH (TH-HELLISH) in time [14,15]. Therefore, what was unique for the structure of HELLISH is that, in principle, the operation of conventional semiconductor light emitters is based on the vertical transport of charge carriers in a forward-biased p-n junction. Incorporating the quantum wells in the active regions of the conventional light-emitting diodes provides better photon and carrier confinement to enhance their efficiency. However, the light emission is confined to a small region of the facet of conventional devices. Therefore, the compatibility in generic integration technology remains a problem. As an alternative to the conventional light emitters, HELLISH contains an undoped QW placed on the n-side of the depletion layer of a p-n junction [9,16]. In fact, with the layer by layer structure of the HELLISH device, it can be thought that there is no significant difference from a conventional heterojunction p-n junction, but HELLISH devices are hot-electron devices and surface-emitting structures. The operation of HELLISH devices is based on longitudinal transport and just requires two ohmic contacts diffused through all the device layers. The longitudinal electric field is applied parallel to the layers and causes the carriers to heat up in their respective channels. The electric field applied to the layers provides heating of the electrons and holes in their respective channels in the barrier layers of a p-n junction. As the applied electric field is increased, electrons and holes in their respective channels become hot. At a given value of the electric field, electrons, which have smaller effective masses and higher mobilities, are excited to higher energy levels than holes. Therefore, they have a higher non-equilibrium temperature than holes. Hot electrons are injected by mainly tunneling into the QW space, resulting in the accumulation of a negative charge in the depletion layer. To preserve charge neutrality, the device self-biases itself, reducing the potential barrier for the holes, and hence excess holes also move into the QW by diffusion, where they recombine with the electrons and

* Corresponding author.
E-mail address: selman.mutlu@istanbul.edu.tr (S. Mutlu).

https://doi.org/10.1016/j.jallcom.2021.160511
0925-8388/

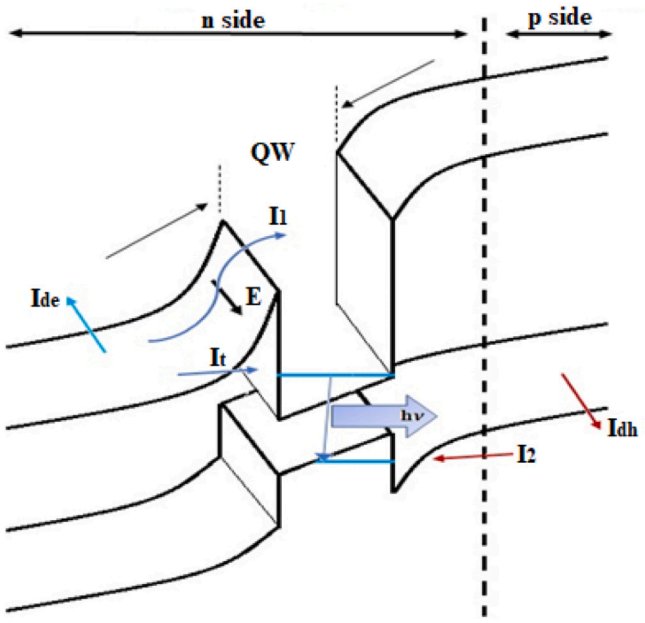

Fig. 1. A schematic illustration of the band diagram of a HELLISH device. *E* is the applied electric field, I_1 and I_t are the currents for the injection of excess electrons by thermionic emission and tunneling, respectively. I_{de} and I_{dh} are electron and hole drift currents, respectively, and I_2 is the hot hole diffusion current in quantum well after the self-biasing of the device.

emit photons at an energy of the bandgap of QW material. The band diagram of the HELLISH structure is given in Fig. 1.

The light emission *via* electroluminescence (EL) from the first HELLISH device was quite broad and weak, and the emission was incoherent [1–4,17]. The first device was basically an AlGaAs p-n junction with a single GaAs QW embedded in the n-side of the depletion layer. Electrons in the n-side, heated by an external electric field, can then tunnel through and thermally surmount the barrier between the n-side and the QW. The accumulation of this negative sheet charge within the depletion layer reduces the potential barrier presented to the holes from the p-side, making it energetically favorable for them to diffuse into the QW. These electrons and holes then recombine, resulting in the EL. The non-equilibrium cases show that as the QW's electron density increases, the depletion length on the n-side increases while on the p-side decreases. This is accompanied by an increase in the potential barrier presented to the electrons outside the depletion region and a decreased potential barrier presented to the holes, thus easing the diffusion of holes into the QW. Therefore, when a longitudinal electric field is applied, *i.e.* electrons are real-space transferred in the well, then the n-side of the device appears to be reverse-biased while the p-side appears to be forward biased.

To enhance the spectral purity of the EL emission and turn the emission characteristic from an LED to a laser, an Ultra-Bright HELLISH (classical HELLISH structure with the bottom DBR stack) and HELLISH-Vertical Cavity Enhanced Surface Emitting Laser (HELLISH-VCSEL, which has a classical HELLISH structure sandwiched with top and bottom DBRs) were demonstrated [5–8,10,12]. One more superiority of HELLISH-based devices is the voltage polarity independent surface light emission, which makes HELLISH devices a candidate to be used as optical logic devices for XOR and NAND logic functions [1,4,6,12,16–18].

In time, some problems showed up with the standard HELLISH design, and the problems that occurred led to the modification of HELLISH as TH-HELLISH [14,19]. The problems observed during the operation of HELLISH devices were i) varying device performance from one device to another, ii) non-uniform light emission across

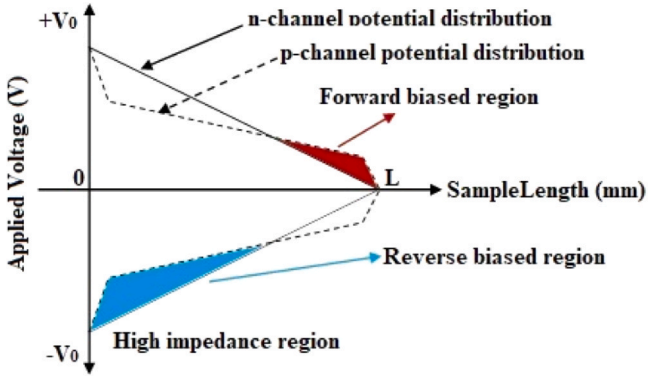

Fig. 2. Potential distribution in n and p channels in the forward and reverse biased regions of a HELLISH device of length L.

HELLISH with higher emission intensity around the cathode region, iii) changing of the intensity of EL according to the applied voltage polarity, and iv) observation EL at the low electric field, which cannot be related to the hot electron effects. Two questions have arisen following these problems: i) are the contacts ohmic for both n- and p-type regions?, and ii) what is the reason for observed low-electric field EL? The answers to these questions led to the design of TH-HELLISH and resulted in the discovery of a novel multifunctional device [19–27]. If the diffused-in contacts are ohmic to n-layer but blocking for the p-layer of the HELLISH device, the regions near the p-contacts become highly resistive, thereby resulting in a non-linear potential distribution over the p-channel of the device as shown in Fig. 2. Therefore, an effective forward biasing of the device is obtained in the vicinity of the cathode. EL intensity may then be dependent on the polarity of the applied voltage. Considering the non-uniform voltage distribution and forward-reversed biased situation as shown in Fig. 5b, the band profile of the HELLISH devices becomes tilted from the drain (+V) to the source regions (0 V), and a quasi-flat band condition is established diagonally as depicted in Fig. 3. In this condition, the carriers' motion is permitted diagonally across the junction as well as the longitudinal transport in the n- and p-channels. On the low electric field regime, due to the established quasi flat band conditions, carriers are transferred into the QW and recombines therein, and in high applied electric fields, hot electron effects control the operation of the HELLISH device [23–25].

To mimic this behavior of the HELLISH devices, the contact structure of HELLISH was modified as separate p- and n-channels, with a longer p-channel and a shorter n-channel. This device was called TH-HELLISH, and it was soon after realized that it has a multifunctional device being as an absorber and emitter

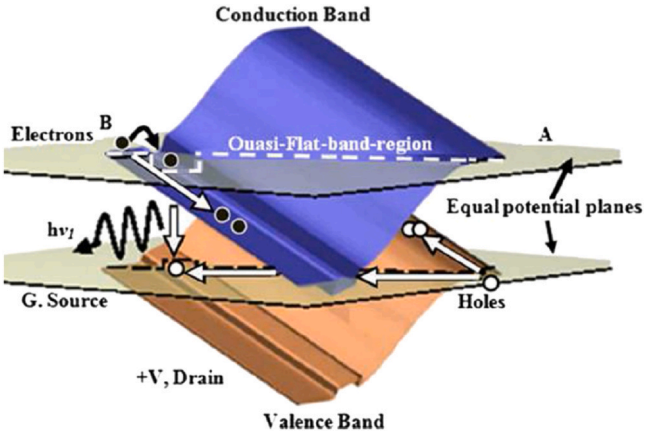

Fig. 3. Quasi-flat band profile of a HELLISH device [23–25].

simultaneously [20,21] as well as a vertical-cavity semiconductor optical amplifier [19,25–27]. A detailed explanation of the operation of TH-HELLISH will be given in the Experimental section. For almost three decades, both HELLISH and TH-HELLISH devices have been adapted to various semiconductor materials to have emission at the desired wavelengths of semiconductor technology in the IR region of the electromagnetic spectrum.

In the present paper, we report a novel blue-light emitting TH-HELLISH device that is based on the InGaN/GaN multi QW structure. High-speed I-V measurements of the device reveal an Ohmic characteristic at both polarities of the applied voltage. Integrated EL measurements reveal the threshold of the applied electric field at around 0.25 kV/cm. The emission wavelength of the device is around 440 ± 1 nm at room temperature. The results indicate that TH-HELLISH can be an alternative to the classical p-n junction based blue-emitting device with its more straightforward fabrication steps and simple device structures. Moreover, using different contact configurations of the device, it can operate as a classical LED and TH-HELLISH.

2. Experimental details

The investigated HELLISH device structure, shown in Table 1, grown on sapphire using metal organic chemical vapor deposition (MOCVD) at Bilkent University Nanotechnology Research Center (NANOTAM). Here, four layers of 3.05 nm thick InGaN quantum wells separated by 13.7 nm thick Si-doped GaN barriers are located on the n-side of a p-n junction. It is a multi-QW structure, which consists of four QWs. The growth temperature was around 1000 °C. For n-type GaN, silicon was the dopant, and for p-type doping, magnesium was preferred because it has the shallowest ionization energy in GaN. The donor density was 1×10^{18} cm^{-3}, and the acceptor density was $1.3x10^{17}cm^{-3}$. The composition of In is 16%, and InGaN is grown on GaN with a compressive strain of 0.01. Because the activation energy for Mg in GaN is relatively high, being 170 meV, we first annealed the sample for having fully ionization of acceptor atoms at 500 °C for 20 min under O_2 ambient [28–30]. To fabricate the TH-HELLISH structure, the n-layer was etched down to a p-type layer. Dry etching is hindered by the strong bond energy in GaN, 8.92 eV/atom, while wet etching is further complicated by its inert chemical nature. We tried several wet etching processes but failed. Therefore, we used reactive ion etching techniques. The top n-type layers were selectively etched 360 nm down to the p-type GaN using ICP-RIE. Contact for the n-type region was formed using Au/Ni/Al/Ti (15/150/40/100 nm) and annealed at 850 °C for 30 s under N_2 ambient [31–34] and for the p-type region, Au/Ni (10/10 nm) was used and annealed at 450 °C for 60 s under O_2 ambient to form NiO_2 [35–39].

The schematic illustration of the fabricated TH-HELLISH structure is given in Fig. 4, together with a contact configuration.TH-HELLISH structure has a shorter n-channel and a longer p-channel, where the n-channel is placed symmetrically concerning the p-channel. The lengths of n- and p-channels are 0.5 mm and 0.9 mm, respectively.

Table 1
Epitaxial structure of TH-HELLISH GaN device.

Repeat	Materials	Layer Thickness (nm)	Dopant	Concentration/cm^3
	GaN	3	Undoped	–
	GaN	112	Si	1.0×10^{18}
	GaN	13.7	Si	1.0×10^{18}
4	InGaN	3.05	Undoped	–
	GaN	13.7	Si	1.0×10^{18}
	GaN	100	Undoped	–
	GaN	307	Mg	1.3×10^{17}
	GaN	1717	Undoped	–
Sapphire (Al_2O_3) Substrate				

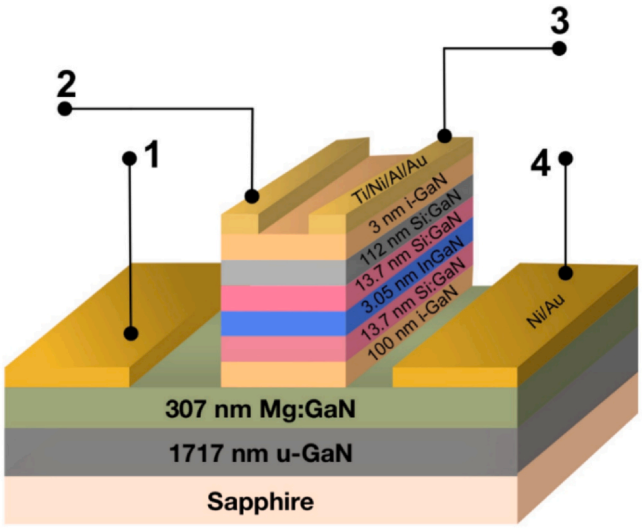

Fig. 4. The schematic representation of the layer structure and contact configuration of the TH-HELLISH-GaN device. There are four ohmic contacts numbered 1, 2, 3, and 4 in this diagram. Contacts numbered 1 and 4 are p-type contacts, while 2 and 3 are n-type contacts.

As seen from the structure of TH-HELLISH, n – and p-regions are isolated from each other. The contacts for n- and p-type regions are Ohmic. Under normal TH-HELLISH operation, contacts 1 and 2 are biased, and contacts 3 and 4 are grounded, as shown in Fig. 5a. The representation of the contact configuration is 12 ± V34G and is called positive polarity. In this contact configuration, contacts 1 and 2 are drain contacts, while 3 and 4 are source contacts. In addition, if the same potential is applied to contacts 3 and 4, contacts 1 and 2 are grounded, the contact configuration is shown as 12G34 ± V, and it is called negative polarity. If we apply forward bias between 1 and/or 3 or 4, the device operates as a conventional p-n junction LED, which operates at vertical transport. Even the contacts on the n- and p-type channels are separated; they are biased at the same voltages according to the device's operating conditions. Fig. 5b shows the potential drop across the device, which mimics the twisted band profile with the problematic HELLISH device shown in Fig. 3. With this structure of the device, emission and absorption regions are interchangeable by just reversing the polarity of the applied voltage; therefore, the device can be operated as a field-effect light emitter and absorber. When the potential is applied to the device in positive polarity, the potential near contact 2 over the length of l_2 is higher in the n-channel than the p-channel ($V_n > V_p$). In this case, the device operates like reverse biased, which acts as a light absorber [20–22]. Simultaneously, the device behaves forward-biased around to contact 3 over the length of l_3, and it also operates as a light emitter [20–22]. In negative polarity, only the locations of the absorption and emission regions change. Therefore, the device has field-effect light emission and absorption characteristics. The position of the contacts provides the nonlinear state in the potential distribution. The contacts' position is labeled as $l_1 = 0$, l_2, l_3, and l_4 for contacts 1, 2, 3, and 4, respectively, in Fig. 5b. The applied voltage distribution along the channels is from contact 2 (l_2) to contact 3 (l_3). The potential difference between n- and p-channels ΔV is a function of device length l and applied voltage V_a. ΔV is the largest at l_2 with maximum reverse bias (V_r) and at l_3 with maximum forward bias (V_f). At the midpoint of the device, ΔV is zero. The ΔV, Vr, and V_f are given by,

$$\Delta V(V_a, l) = -\frac{XV_a}{l_2 - l_3}[2l - (l_2 + l_3)] \ , \ l_2 < l < l_3 \quad (1)$$

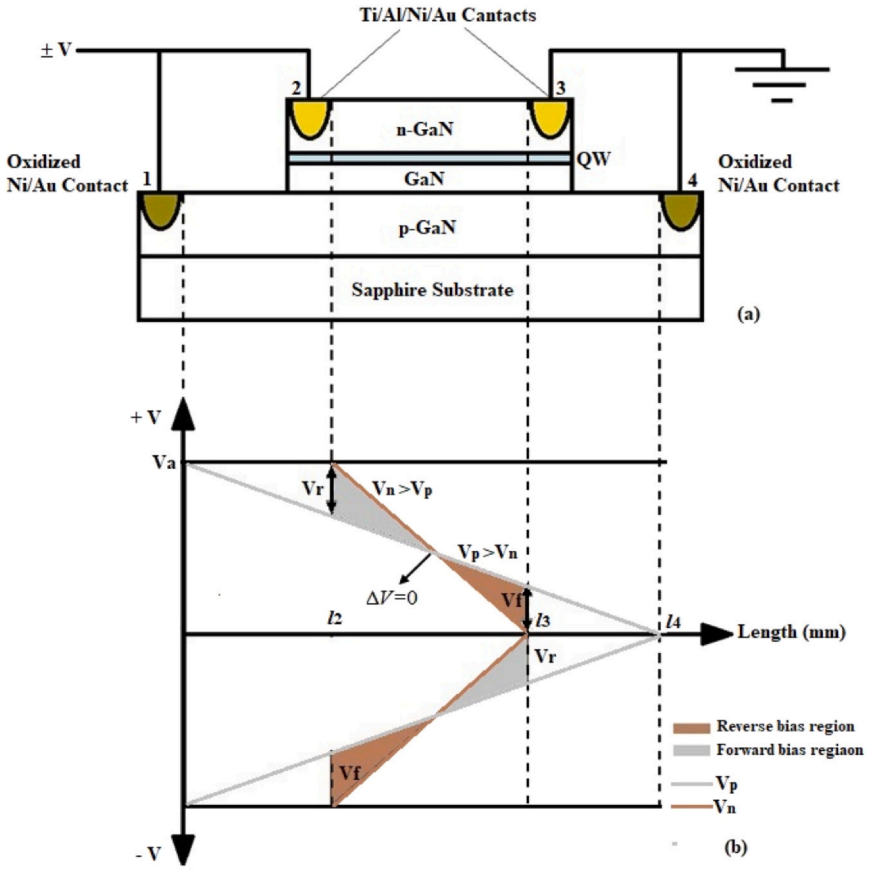

Fig. 5. a) Schematic illustration of the TH-HELLISH structure and configuration of the contacts. Under normal operating conditions, the device is biased at the contacts 1 and 2 with ± V, while 3 and 4 are grounded. b) Potential distribution along with the n (brown line) and p (gray line) channels of the device. In the region $V_n > V_p$, the device is effectively reverse biased; and in the region $V_p > V_n$, it is effectively forward biased. V_r and V_f are the maximum reverse bias and forward bias within the junction, respectively. V_a is the applied voltage. ΔV is the voltage difference [20–22,25,27].

$$V_{r,l_2} = -\frac{l_4 - (l_3 - l_2)}{2l_4} V_a = -XV_a \ , \quad l = l_2 \tag{2}$$

$$V_{f,l_3} = XV_a \ , \quad l = l_3 \tag{3}$$

where, $X = [l_4 - (l_3 - l_2)]/2l_4$ is dimensionless TH-HELLISH parameter [20].

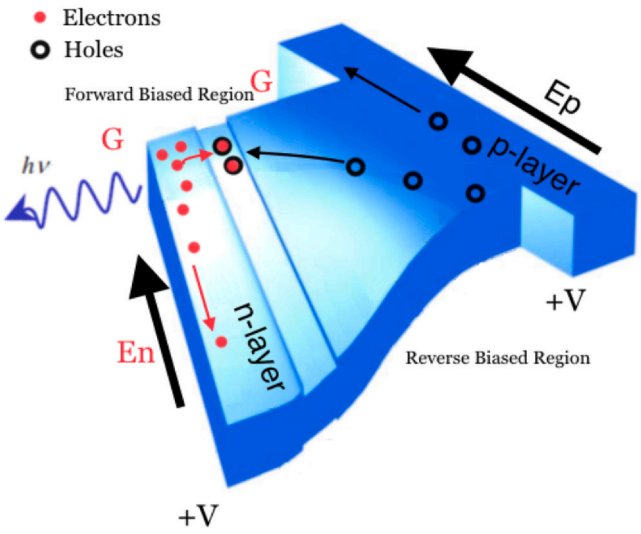

Fig. 6. The twisted band profile of TH-HELLISH.

Fig. 6 shows the twisted band profile of TH-HELLISH. The twisted band profile results from the forward and reverses biased areas along the junction, as shown in Fig. 5b. The flat band condition is established at the cathode, and the reverse bias region occurs at the anode.

The I-V and spectral EL measurements were carried out using high-speed pulsed measurements systems, which includes a pulse generator (Avtech AVRZ-5) at 300 ns pulse width and 2.04 ms pulse repetition rate with a duty cycle 0.0147 to apply voltage, a monochromator with a 1/3 focal length (Acton SR-2300i) is used to disperse the emitted light, a GaAs PMT (Hamamatsu R3896) accompanied with a boxcar (Stanford Research System SR250) to detect the signal, and an oscilloscope (1.5 GHz LeCroy 715Zi) to monitor applied voltage and voltage across the load resistance. Integrated EL was collected directly with PMT without using a monochromator. A 50 Ohm load resistance was connected in serial with the device to have resistance match with the oscilloscope, and a voltage drop on the load resistance was measured, then the sample voltage was determined during measurements. All of the measurements were carried out at room temperature.

3. Experimental results

The current-electric field (I-E) characteristic in Fig. 7 exhibits a linear behavior at both polarities and, therefore, all contacts to the n- and p-layers are Ohmic.

The measured integrated EL intensity as a function of an applied electric field for both polarities is illustrated in Fig. 8 at room temperature. The threshold electric field (E_{th}) and the corresponding threshold voltage (V_{th}) are obtained as 0.25 kV/cm and 12.5 V,

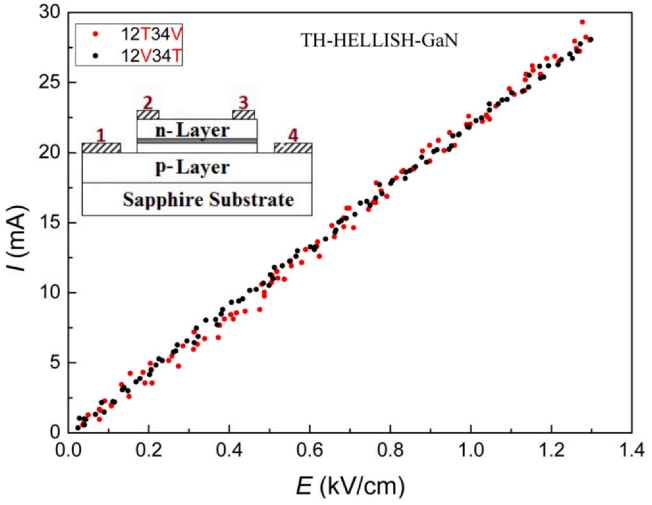

Fig. 7. The current-electric field (I-E) characteristics for positive (12V34G) and negative polarities (12G34V) at room temperature.

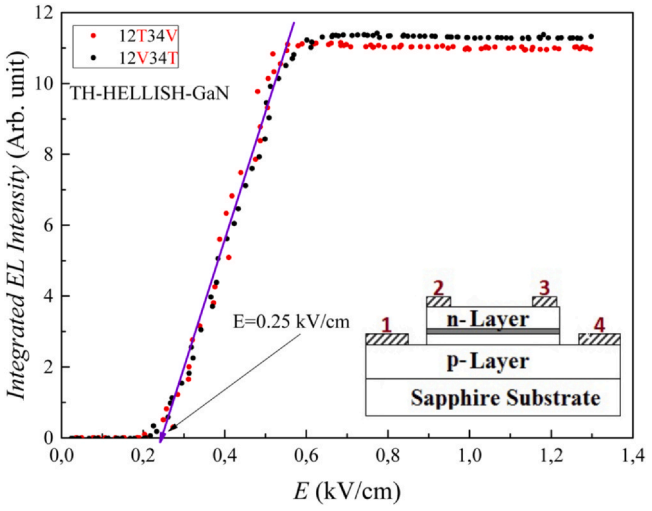

Fig. 8. Integrated EL intensity *versus* applied electric field for both polarities at room temperature.

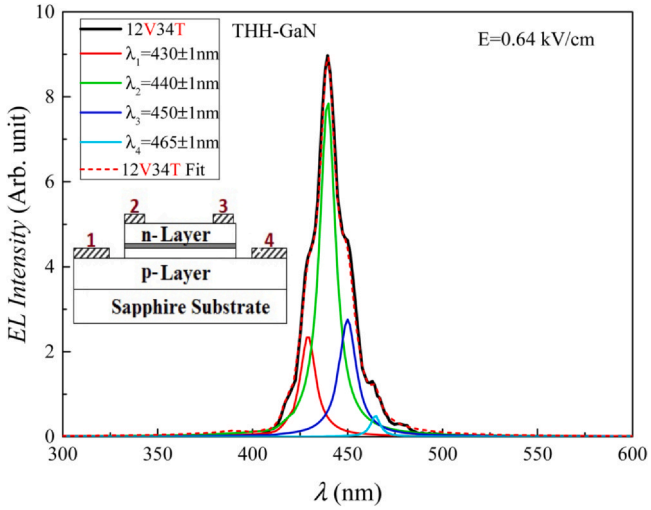

Fig. 10. The convolution of the EL spectrum into peaks in an applied electric field of 0.65 kV/cm.

respectively. It is clearly seen that the light intensity is independent of the applied voltage polarity because both polarities show the same behavior. Therefore, the TH-HELLISH-GaN device exhibits an XOR function. Integrated EL intensity saturates at around 0.56 kV/cm.

In Fig. 9a and b, EL spectra are given as a function of an applied electric field for positive polarity and negative polarity, respectively. EL measurements are performed in the range of 300–600 nm wavelength, and 0.11–0.64 kV/cm applied electric field for both polarities at room temperature. The center peak of the observed EL spectra is at 440 ± 1 nm. The inset in Fig. 9 reveals that EL intensity linearly increases with an increasing electric field. In addition, there is no shift of the emission wavelength due to the applied electric field in the EL spectra observed, and the characteristic of EL spectra exhibits similar behavior in both polarities. The photographs of the surface-emission of a TH-HELLISH-GaN device are captured at an applied electric field of 0.64 kV/cm for both polarities, as shown in the inserted figure in Fig. 9. It is clear that the device surface emission is indeed from the cathode region for both polarities, which is in good agreement with the predictions of potential distribution in n- and p-channels as shown in Fig. 5b [20–22,25,27].

The conclusion of the central EL peak into peaks in an electric field of 0.65 kV/cm are shown in Fig. 10. Four peaks are obtained. The

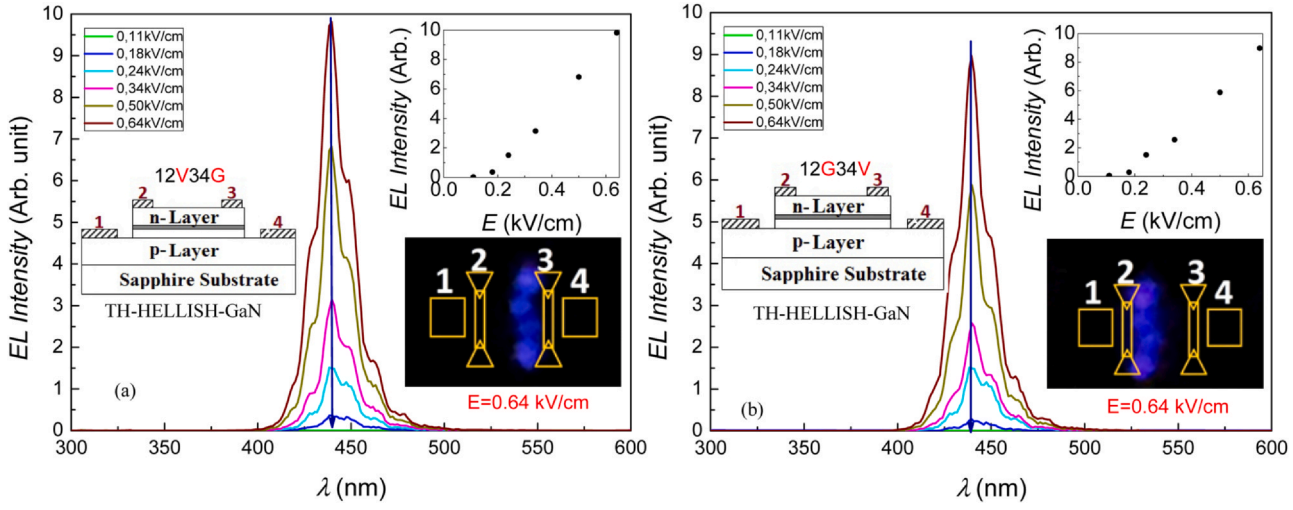

Fig. 9. EL spectra depending on the applied electric field and surface emission photographs for **a.** positive polarity **b.** negative polarity at room temperature. The inset at the top shows the changes in EL intensity.

first emission peak with a wavelength of 430 ± 1 nm is often observed in the spectra of Si-doped n-type GaN grown by MOCVD or HVPE, attributed to transitions from the shallow donor level or conduction band to the roughly deep acceptor level having ionization energy [40]. The second emission peak is centered on 440 ± 1 nm, which corresponds to the transition between the first electron subband and the first light hole subband (Ee1-Elh1) in GaN QW, which agrees with the reported values for GaN QW structures [41,42]. The third peak is at 450 ± 1 nm and corresponds to the first energy level of the electron-first energy level of the heavy hole (Ee1-Ehh1) transition of the GaN QW [43]. The last emission peat at 465 ± 1 nm is thought to be a radiative transition from the first energy level of an electron (Ee1) to a trap level formed by the clustering of indiums in the structure [40,44–46].

The operation performance of the TH-HELLISH-GaN device can be developed by minimizing the dimensions of the device; in this way, the higher electrical fields can be obtained by using much smaller voltages. Furthermore, the alloy concentration can be changed to improve the device. Therefore, designed devices radiate at a different wavelength. The Ga rich (x > 0.5) $In_{1-x}Ga_xN$ alloys can be used as light emitters with wavelength ranging from about 360–600 nm. However, recent growth techniques have made it possible to extend this range to NIR wavelengths by increasing the In composition (indium rich) $In_{1-x}Ga_xN$, leading to single-compound-based light emitters to cover a wide range of the electromagnetic spectrum from ultraviolet to near-infrared. Finally, more intensity and narrower emission peak can be obtained by adding suitable DBR layers for the device structure.

4. Conclusions

We have reported a novel blue light-emitting TH-HELLISH device based on an InGaN/GaN multi QW structure. The light emission of the TH-HELLISH-GaN device is observed to be around 440 ± 1 nm at room temperature. It is observed that the device's emission wavelength and light intensity are independent of the polarity of the applied electrical field. Therefore, the device can be used for the XOR optical logic gate concerning applied voltage. The threshold of the applied electrical field for the operation of the device is obtained around 0.25 kV/cm, which corresponds to 12.5 V. Our results reveal that, with a more straightforward structure, and easier fabrication route, and multifunctional GaN-base, TH-HELLISH is an excellent alternative to the conventional blue LEDs and a versatile device to have a potential to be utilized as optical logic gates. The operation performance of the TH-HELLISH-GaN device can be developed by minimizing the dimensions of the device; in this way, the higher electrical fields can be obtained by using much smaller voltages.

CRediT authorship contribution statement

Selman Mutlu: Investigation, Visualization, Data curation, Formal anaysis, Writing - original draft. **Ayse Erol:** Writing - original draft, Resources, Validation. **Engin Arslan:** Writing - review & editing. **Ekmel Ozbay:** Resources. **Sefer Bora Lisesivdin:** Formal analysis, Validation. **Engin Tiras:** Conceptualization, Supervision, Writing - review & editing.

Declaration of Competing Interest

The authors declare that they have no known competing financial interests or personal relationships that could have appeared to influence the work reported in this paper.

Acknowledgements

This work was supported by the Scientific Research Projects Coordination Unit of Istanbul University (project number BEK-2017–24514) and the Scientific Research Projects Coordination Unit of Anadolu University (project number 1502F069).

References

[1] A. Straw, N. Balkan, A. O'Brien, A. Da Cunha, R. Gupta, M. Arikan, Hot electron light-emitting and lasing semiconductor heterostructures - type 1, Superlattices Microstruct. 18 (1) (1995) 33–43.
[2] R. Gupta, N. Balkan, A. Teke, A. Straw, A. Cunha, Hot electron light-emitting semiconductor heterostructure device-type 2, Superlattices Microstruct. 18 (1) (1995) 45–51.
[3] N. Balkan, A. Teke, R. Gupta, A. Straw, J.H. Wolter, W. Van Der Vleuten, Tunable wavelength hot electron light emitter, Appl. Phys. Lett. 67 (7) (1995) 935–937.
[4] N. Balkan, A. A. da Cunha, A. O'Brien, A. Teke, R. Gupta, A. Straw, M.C. Arikan, Hot Carriers in Semiconductors, edited by K. Hess, J. P. Leburton, and U. Ravaioli ~Plenum, 1996.
[5] A. O'brien, N. Balkan, A. Boland-Thoms, M. Adams, A. Bek, A. Serpengüzel, A. Aydinli, J. Roberts, Super-radiant surface emission from a quasi-cavity hot electron light emitter, Opt. Quantum Electron. 31 (2) (1999) 183–190.
[6] A. O'Brien, N. Balkan, J. Roberts, Ultra bright surface emission from a distributed Bragg reflector hot electron light emitter, Appl. Phys. Lett. 70 (3) (1997) 366–368.
[7] A. O'Brien-Davies, N. Balkan, A. Boland-Thoms, M.J. Adams, J. Roberts, Hellish-VCSEL: a hot electron laser, Turk. J. Phys. 23 (4) (1999) 681–688.
[8] N. Balkan, A. Serpengüzel, A. O'Brien-Davies, I. Sökmen, C. Hepburn, R. Potter, M.J. Adams, J.S. Roberts, VCSEL structure hot electron light emitter, Mater. Sci. Eng. B Solid-State Mater. Adv. Technol. 74 (1) (2000) 96–100.
[9] A. Erol, N. Balkan, M.Ç. Arıkan, A. Serpengüzel, J. Roberts, Temperature dependence of the threshold electric field in a hot electron VCSEL, IEE Proc. Optoelectron. 152 (6) (2003) 299–320.
[10] R. Sceats, A. Dyson, A. Boland-Thoms, N. Balkan, M.J. Adams, C.C. Button, Hot electron GaInAsP/InP surface emitter, Phys. Simul. Optoelectron. Devices VIII 3944 (2000) 882.
[11] R. Sceats, C.J. Hepburn, R. Potter, A. Dyson, N. Balkan, M.J. Adams (n.d.) 1. 5 um Surface Emission From GaInAsP/InP HELLISH Structures. 4283, 2001, 723–732.
[12] R. Sceats, A. Dyson, C. J. Hepburn, R. J. Potter, A. Boland-Thoms, N. Balkan, G. Hill, C. C. Button, S. Pinches, Hot electron light emission from GaInAsP/InP structures with distributed Bragg reflectors, Phys. E Low Dimens. Syst. Nanostruct. 17 (1–4) (2003) 607–609.
[13] F. Chaqmaqchee, S. Mazzucato, N. Balkan, 2011. 1.3 μm dilute nitride HELLISH-VCSOAs. International Conference on Transparent Optical Networks. 1–3.
[14] J.Y. Wah, N. Loubet, R.J. Potter, S. Mazzucato, A. Arnoult, H. Carrère, E. Bedel, X. Marie, N. Balkan, Bi-directional field effect light emitting and absorbing heterojunction with GaInNAs at 1250nm, IEE Proc. Optoelectron. 150 (2003) 72–74.
[15] F.A.I. Chaqmaqche, N. Balkan, Ga0.35In0.65 N0.02As0.08/GaAs bidirectional light-emitting and light-absorbing heterojunction operating at 1.3 μm, Nanoscale Res. Lett. 9 (37) (2014) 37.
[16] N. Balkan, Non-linear carrier dynamics in hot electron vertical cavity surface emitting laser, Phys. B Condens. Matter 272 (1–4) (1999) 480–483.
[17] N. Balkan, A. Teke, R. Gupta, Tunable wavelength light emission from longitudinally biased p-GaAs/n-Ga1-xAlxAs junction containing GaAs quantum wells: non-linear dynamics, Phys. E Low Dimens. Syst. Nanostruct. 4 (4) (1999) 300–315.
[18] H. Naundorf, R. Gupta, E. Schöll, A model for hot electron light emission from semiconductor heterostructures, Semicond. Sci. Technol. 13 (6) (1998) 548–556.
[19] F.A.I. Chaqmaqchee, Optical amplification in dilute nitride hot electron light emission–VCSOAs devices, Arab. J. Sci. Eng. 40 (7) (2015) 2111–2115.
[20] J.Y. Wah, N. Balkan, R.J. Potter, J.S. Roberts, The operation of a wavelength converter based on a field effect light emitting and absorbing heterojunction, Phys. Status Solidi A Appl. Res. 196 (2) (2003) 496–503.
[21] J.Y. Wah, N. Balkan, A. Boland-Thoms, J.S. Roberts, Hot electron light emission and absorption processes in a Top Hat structured bi-directional wavelength converter/amplifier, Phys. E Low Dimens. Syst. Nanostruct. 17 (1–4) (2003) 610–612.
[22] C.J. Hepburn, J.Y. Wah, A. Boland-Thoms, N. Balkan, GaInNAs and GaAs, top-hat vertical-cavity semiconductor optical amplifier (VCSOA) based on longitudinal current transport, Phys. Status Solidi C Conf. 2 (8) (2005) 3096–3099.
[23] J.Y. Wah, N. Balkan, 2005. Low field operation of hot electron light emitting devices: quasi-flat-band model. 152 (6), 299–320.
[24] F.A. Chaqmaqchee, S. Mazzucato, M. Oduncuoglu, N. Balkan, Y. Sun, M. Gunes, M. Hugues, M. Hopkinson, Gainnas-based hellish-vertical cavity semiconductor optical amplifier for 1.3 μm operation, Nanoscale Res. Lett. 6 (2011) 1–7.
[25] F.A.I. Chaqmaqchee, N. Balkan, J.M.U. Herrero, Top-Hat HELLISH-VCSOA for optical amplification and wavelength conversion for 0.85 to 1.3μm operation, Nanoscale Res. Lett. 7 (2012) 1–6.
[26] F.A.I. Chaqmaqche, S. Mazzucato, N. Balkan, M. Hugues, M. Hopkinson, Gain characteristic of dilute nitride HELLISH-VCSOA for 1.3 μm wavelength operation, Phys. Status Solidi C Curr. Top. Solid State Phys. 10 (4) (2013) 564–566.

[27] F.A.I. Chaqmaqchee, N. Balkan, 2014. Ga0.35In0.65 N0.02As0.08/GaAs bidirectional light-emitting and light-absorbing heterojunction operating at 1.3 μm. 5–9.
[28] T.C. Wen, S.C. Lee, W.I. Lee, T.Y. Chen, S.H. Chan, J.S. Tsang, Activation of p-type GaN in a pure oxygen ambient, Jpn. J. Appl. Phys. Part 2 Lett. 40 (5 B) (2001) 38–41.
[29] C.H. Kuo, S.J. Chang, Y.K. Su, L.W. Wu, J.K. Sheu, C.H. Chen, G.C. Chi, Low temperature activation of Mg-doped GaN in O2 ambient, Jpn. J. Appl. Phys. 41 (2 A) (2002) L112–L114.
[30] J. Ho, C. Jong, C.C. Chiu, C. Huang, K. Shih, L. Chen, et al. , 2004. Low-resistance ohmic contacts to p-type GaN achieved by the oxidation of Ni / Au films Low-resistance ohmic contacts to p-type GaN achieved by the oxidation of Ni / Au films. 4491 (1999).
[31] M.E. Lin, Z. Ma, F.Y. Huang, Z.F. Fan, L.H. Allen, H. Morkoç, Low resistance ohmic contacts on wide band-gap GaN, Appl. Phys. Lett. 64 (8) (1994) 1003–1005.
[32] B. Boudart, S. Trassaert, X. Wallart, J.C. Pesant, O. Yaradou, D. Théron, Y. Crosnier, H. Lahreche, F. Omnes, Comparison between TiAl and TiAlNiAu ohmic contacts to n-type GaN, J. Electron. Mater. 29 (5) (2000) 603–606.
[33] Z.X. Qin, Z.Z. Chen, Y.Z. Tong, X.M. Ding, X.D. Hu, T.J. Yu, G.Y. Zhang, Study of Ti/Au, Ti/Al/Au, and Ti/Al/Ni/Au ohmic contacts to n-GaN, Appl. Phys. A Mater. Sci. Process. 78 (5) (2004) 729–731.
[34] K. Singh, A. Chauhan, M. Mathew, R. Punia, S.S. Meena, N. Gupta, R.S. Kundu, Formation of non-alloyed Ti/Al/Ni/Au low-resistance ohmic contacts on reactively ion-etched n-type GaN by surface treatment for GaN light-emitting diodes applications, Appl. Phys. A 125 (1) (2019) 24.
[35] H.W. Jang, S.Y. Kim, J.L. Lee, Mechanism for ohmic contact formation of oxidized Ni/Au on p-type GaN, J. Appl. Phys. 94 (3) (2003) 1748–1752.
[36] C.T. Lee, Y.J. Lin, T.H. Lee, Mechanism investigation of NiOx in Au/Ni/p-type GaN ohmic contacts annealed in air, J. Electron. Mater. 32 (5) (2003) 341–345.
[37] P.P. Cheng, X.C. Liu, P.F. Ma, C. Gao, J.L. Li, Y.Y. Lin, W. Shao, S. Han, B. Zhao, L.M. Wang, J.Z. Fu, L.X. Meng, Q. Li, Q.Z. Lian, J.J. Xia, Z.Q. Qi, iPSC-MSCs combined with low-dose rapamycin induced islet allograft tolerance through suppressing Th1 and enhancing regulatory T-cell differentiation, Stem Cells Dev. 24 (11) (2015) 1793–1804.
[38] J. Chen, W.D. Brewer, Ohmic Contacts on p-GaN, Adv. Electron. Mater. 1 (8) (2015) 1–7.
[39] C. Zhao, H. Wang, J. Xiong, J. Wu, Temperature dependence and high-temperature stability of the annealed Ni/Au ohmic contact to p-type GaN in air, J. Electron. Mater. 45 (4) (2016) 2087–2091.
[40] M.A. Reshchikov, H. Morkǫ, Luminescence properties of defects in GaN, J. Appl. Phys. 97 (6) (2005) 061301.
[41] Z.Z. Chen, P. Liu, S.L. Qi, K. Xu, Z.X. Qin, Y.Z. Tong, T.J. Yu, X.D. Hu, G.Y. Zhang, Origins of double emission peaks in electroluminescence spectrum from InGaN/GaN MQW LED, Pan Tao Ti Hsueh Pao Chin. J. Semicond. 28 (7) (2007) 1121–1124.
[42] H. Ekinci, V.V. Kuryatkov, C. Forgey, A. Dabiran, R. Jorgenson, S.A. Nikishin, Properties of InGaN / GaN MQW LEDs grown by MOCVD with and without hydrogen carrier gas, Vaccum 148 (2018) 168–172.
[43] M. Yuan, H. Li, J. Zeng, H. Fan, Q. Dai, S. Lan, et al., 2014. Multiple quantum wells excited by 2. 48- μ m femtosecond laser pulses. 39 (12), 3555–3558.
[44] R.A. Arif, H. Zhao, Y.K. Ee, N. Tansu, Spontaneous emission and characteristics of staggered InGaN quantum-well light-emitting diodes, IEEE J. Quantum Electron. 44 (6) (2008) 573–580.
[45] T.V. Bezyazychnaya, D.M. Kabanau, V.V. Kabanov, Y.V. Lebiadok, A.G. Ryabtsev, G.I. Ryabtsev, V.M. Zelenkovskii, S.K. Mehta, Influence of vacancies on indium atom distribution in InGaAs and InGaN compounds, Lith. J. Phys. 55 (1) (2015) 10–16.
[46] F. Zhang, M. Ikeda, K. Zhou, Z. Liu, J. Liu, S. Zhang, H. Yang, Injection current dependences of electroluminescence transition energy in InGaN/GaN multiple quantum wells light emitting diodes under pulsed current conditions, J. Appl. Phys. 118 (3) (2015) 033101.